# Zinc-finger E-box-binding homeobox 1 alleviates acute kidney injury by activating autophagy and the AMPK/mTOR pathway

DEHUA SUN[1-3], XIAOHUA LIU[4], LIJUAN ZHU[5] and BIN ZHANG[1-3]

[1]Department of Critical Care Medicine, The First Affiliated Hospital of Shandong First Medical University (Shandong Provincial Qianfoshan Hospital), [2]Shandong Medicine and Health Key Laboratory of Emergency Medicine, [3]Shandong Institute of Anesthesia and Respiratory Critical Medicine, Jinan, Shandong 250014; [4]Department of Gastroenterology, The People's Hospital of Jimo, Qingdao, Shandong 266200; [5]Emergency Intensive Care, Huizhou Central People's Hospital, Huizhou, Guangdong 516000, P.R. China

Received March 25, 2020; Accepted January 27, 2021

DOI: 10.3892/mmr.2021.12082

**Abstract.** Zinc-finger E-box-binding homeobox 1 (ZEB1) is involved in epithelial-mesenchymal transition. In the present study, the protective effect of ZEB1 on acute kidney injury (AKI) was explored. The cecal ligation and puncture (CLP) method was performed to establish the AKI model in rats. ZEB1 expression, blood urea nitrogen (BUN) and serum creatinine (SCr) levels, inflammation [interleukin (IL)-1β, IL-6, and tumour necrosis factor-α], phosphorylated AMP-activated protein kinase (p-AMPK) and phosphorylated mammalian target of rapamycin (p-mTOR) expression, and histopathological changes in CLP-induced AKI rats were assessed. AMPK inhibitor dorsomorphin (DM) was intraperitoneally injected to determine the effect of ZEB1 on AKI and the regulatory mechanism involving the AMPK/mTOR pathway. CLP downregulated ZEB1 expression, increased BUN and SCr levels, promoted inflammation and apoptosis, and increased the acute kidney score in the kidney tissues of CLP-induced AKI rats. Autophagy and the AMPK/mTOR pathway were blocked in CLP-induced AKI rats. ZEB1 overexpression inhibited inflammation and apoptosis, reduced BUN and SCr levels, and activated autophagy and the AMPK/mTOR pathway in CLP-induced AKI rats. The protective effect of ZEB1 overexpression on AKI was reversed by DM. Thus, ZEB1 was revealed to alleviate CLP-induced AKI by activating autophagy and the AMPK/mTOR pathway.

*Correspondence to:* Dr Bin Zhang, Department of Critical Care Medicine, The First Affiliated Hospital of Shandong First Medical University (Shandong Provincial Qianfoshan Hospital), 16766 Jingshi Road, Jinan, Shandong 250014, P.R. China
E-mail: zhangbin1942020@163.com

*Key words:* Zinc-finger E-box-binding homeobox 1, acute kidney injury, AMPK/mTOR signalling pathway, apoptosis, autophagy

## Introduction

Acute kidney injury (AKI) refers to an acute decrease or even loss of kidney function within hours that is caused by a variety of factors, including sepsis, ischaemia, and nephrotoxicity (1). According to the location and aetiology of the lesion, AKI is classified as prerenal AKI, renal parenchymal or renal vascular disease-related AKI, and postrenal AKI (2). Sepsis often leads to septic shock and multiple organ dysfunction, and AKI is one of the common lethal complications of sepsis (3,4). Acute peritoneal dialysis and continuous renal replacement therapy are the most common clinical treatment methods for AKI (5,6). Although numerous existing studies have focused on the treatment of AKI, a novel treatment protocol remains to be established.

Autophagy degrades and recycles damaged macromolecules and organelles to maintain the stability of the intracellular environment. Autophagy is activated under stress conditions, including endoplasmic reticulum stress, oxidant injury, cell starvation, hypoxia, and nutrient deprivation (7,8). Most of the stress conditions for activating autophagy are involved in the pathogenesis of AKI (7,8). The reactive oxygen species (ROS) and oxidative stress involved in AKI trigger autophagy in animal cells and tissues, resulting in aggravated kidney injury (9). Autophagy can antagonise apoptosis, and the inhibition of autophagy aggravates sepsis-induced AKI (10,11). Autophagy in the stress response is mediated by diverse signalling pathways, such as the phosphoinositide 3-kinase (PI3K)/protein kinase B (AKT), ROS/c-Jun N-terminal kinase (JNK), and AMP-activated protein kinase (AMPK)/mammalian target of rapamycin (mTOR) pathways (12-15). The AMPK/mTOR pathway plays a major role in AKI autophagy. Previous findings have indicated that recombinant human erythropoietin suppresses lipopolysaccharide (LPS)-induced cell apoptosis in AKI rats via AMPK-mediated autophagy (16). Furthermore, NAD-dependent deacetylase sirtuin-3 alleviates AKI by inducing autophagy via regulation of the AMPK/mTOR pathway (17).

Zinc-finger E-box-binding homeobox 1 (ZEB1), a member of the ZEB family, plays a critical role in epithelial-mesenchymal transition (EMT) (18-20). In addition, numerous studies

have demonstrated that ZEB1 plays a major role in a variety of diseases, such as invasive endometriosis, cerebral arterial thrombosis, brain ischaemia, and ischaemic stroke (21-24). A previous study reported that ZEB1 overexpression plays a protective role in brain ischaemia (23). ZEB1 overexpression has been confirmed to ameliorate brain damage after acute ischaemic stroke by reducing central nervous system inflammation (24). Additionally, ZEB1 protects skeletal muscle from damage and accelerates skeletal muscle regeneration (25). However, studies of ZEB1 effects on AKI are limited.

In the present study, an AKI model in rats was established using the cecal ligation and puncture (CLP) method. The autophagy, inflammation, apoptosis, and injury of kidney tissues were evaluated in CLP-induced AKI rats. In addition, the regulatory mechanism of ZEB1 involving the AMPK/mTOR pathway was analysed in CLP-induced AKI rats. The present study findings may provide a new theoretical foundation for the treatment of AKI.

## Materials and methods

*Establishment of the adenovirus (Ad) vector*. The ZEB1 fragment was amplified and inserted into the overexpression vector pcDNA 3.1 (promoter CMV; Invitrogen; Thermo Fisher Scientific, Inc.) to construct pcDNA-ZEB1. Thereafter, the fragment was sub-cloned into the Ad vector pAdTrack-CMV (promoter CMV; Agilent Technologies, Inc.) to construct Ad-ZEB1. The empty pAdTrack-CMV vector was used as a negative control (Ad-NC).

*Rat model of CLP-induced AKI*. A total of 70 male Sprague-Dawley rats (age, ~8 weeks; weight, 250±10 g) were obtained from Laboratory Animal Center of Southern Medical University (Guangzhou, China). All rats in experiments were provided free access to water and normal rat chow and were acclimatized for 7 days at 24˚C, 60±10% humidity and 12-h light/dark cycles. Rats were randomly divided into seven groups (n=10 in each group): Blank, sham, CLP, CLP + Ad-NC, CLP + Ad-ZEB1, CLP + Ad-NC + dorsomorphin (DM; Sigma-Aldrich: Merck KGaA), and CLP + Ad-ZEB1 + DM. CLP-induced AKI was constructed in the rats as previously described (26). Briefly, all rats fasted for 12 h before CLP surgery. The rats underwent 1 cm midline laparotomy under anaesthesia (intraperitoneal injection of 50 mg/kg pentobarbital sodium). The caecum was ligated with a 4-0 silk suture at 1 cm from the end. A 22-gauge needle was used to puncture the caecum with two holes close to the ligation site. A small amount of faeces was squeezed out through the two holes to induce sepsis. Sham rats only underwent laparotomy and bowel manipulation. Ad-ZEB1 and Ad-NC ($2x10^7$ TU/ml) were intravenously injected into the tail of rats in the CLP + Ad-NC and CLP + Ad-ZEB1 groups, respectively, 2 days before CLP. In the CLP + Ad-NC + DM group, rats were intravenously injected with Ad-NC caudally and intraperitoneally injected with DM (20 mg/kg) before CLP. In the CLP + Ad-ZEB1 + DM group, rats were intravenously injected with Ad-ZEB1 caudally and intraperitoneally injected with DM (20 mg/kg) before CLP. The rats were anaesthetised by intraperitoneal injection of pentobarbital sodium (50 mg/kg) and sacrificed by cervical dislocation. All experimental protocols were approved by the Ethics Committee of the First Affiliated Hospital of Shandong First Medical University. All procedures were performed in accordance with ethical standards and laboratory care and use guidelines of the First Affiliated Hospital of Shandong First Medical University.

*Assessment of renal function*. Blood samples were collected from the inferior vena cava of the rats. The blood urea nitrogen (BUN) and serum creatinine (SCr) levels were measured using an automated biochemical analyser (TBA-40FR; Toshiba). The 24-h urine volume was measured gravimetrically. Urinary sodium was measured with an ion-selective electrode (Nova Biomedical), and urine osmolality was measured using a freezing-point osmometer (3D3; Advanced Instruments, Inc.). The mean arterial pressure (MAP) was measured using a non-invasive blood pressure monitoring system (ALC-NIBP; Alcott Biotech Co., Ltd.). The renal blood flow (RBF) was recorded using PowerLab (model 8S) and LabChart software (version 5.1.1, ADInstruments PTY, Inc.) and calculated as the average flow during the first 10-sec interval of each minute over a 10-min period after stabilised flow.

*Sepsis score*. After treatment for 24 h, the sepsis in rats was evaluated according to Shrum's scoring system (27). The scores included appearance, consciousness, activity, response to stimulus, eyes, and respiration rate and quality (0-4 points). A higher total score indicates greater sepsis severity.

*Hematoxylin and eosin (H&E) staining*. The kidney tissues were collected and fixed in 4% formaldehyde solution for 24 h at room temperature. Paraffin-embedded kidney tissues were sectioned into 5-$\mu$m-thick sections. The sections were deparaffinised with xylene, dehydrated with graded ethanol, and stained with H&E for 15 min at room temperature. Histopathological changes of the kidney tissues were observed under a light microscope at a magnification of x200. Five fields were selected randomly for each animal. The degree of kidney damage was assessed according to the following criteria (28): 0, normal; 1, <25%; 2, 25-50%; 3, 50-75%; and 4, 75-100%.

*Terminal deoxynucleotidyl transferase dUTP nick end labeling (TUNEL) assay*. Cell apoptosis was detected using a TUNEL kit (TransGen Biotech Co., Ltd.). In brief, the samples were fixed with 4% paraformaldehyde at 4˚C for 4 h. Following this, samples were treated with 3% hydrogen peroxidase and incubated in a labeling reaction mixture comprised of terminal deoxynucleotidyl transferase and deoxynucleotides overnight at 4˚C. Sections were then subjected to further incubation with horseradish peroxidase (1:500; Shanghai Macklin Biochemical Co., Ltd.) for 30 min and treatment with 3,3'-diaminobenzidine for 15 min at 37˚C in the dark. Reactions were stopped with running water and counterstaining was performed with hematoxylin at 37˚C for 10 min. Following dehydration with a graded ethyl alcohol series and xylene treatment, tissue samples were mounted on coverslips with neutral gum. Apoptotic nuclei appeared as dark brown dots. TUNEL-positive cells were counted in five randomly selected regions (magnification, x200), and the percentage of TUNEL-positive cells was calculated using Image-Pro Plus software (Media Cybernetics, Inc.).

Table I. Kidney function-associated parameters in rats.

| Parameters | Blank | Sham | CLP |
|---|---|---|---|
| Urine volume (ml/24 h) | 14.78±2.23 | 15.13±1.12 | 34.61±2.34[a] |
| Urine osmolality (mOsm/kg) | 818.29±62.46 | 856.45±57.28 | 349.59±39.62[a] |
| Urine sodium (%) | 0.11±0.02 | 0.13±0.01 | 1.59±0.48[a] |
| MAP (mmHg) | 112.48±11.77 | 106.62±10.33 | 87.46±7.37[a] |
| RBF (ml/min/g) | 4.28±0.46 | 4.34±0.28 | 2.46±0.13[a] |

[a]P<0.01 vs. blank. MAP, mean arterial pressure; RBF, renal blood flow; CLP, cecal ligation and puncture.

*Reverse transcription-quantitative polymerase chain reaction (RT-qPCR).* Total RNA from kidney tissues was extracted using TRIzol reagent (Invitrogen; Thermo Fisher Scientific, Inc.) according to the manufacturer's instructions. For cDNA synthesis, 2 $\mu$g of total RNA was reverse transcribed using the PrimeScript™ RT Reagent Kit with gDNA Eraser (Perfect Real Time; Takara Bio, Inc.). qPCR was carried out using SYBR-Green PCR Master Mix (Takara Bio, Inc.) on a Bio-Rad Real-Time PCR instrument (Bio-Rad Laboratories, Inc.). The following thermocycling conditions were used for qPCR: Initial denaturation at 95˚C for 3 min; followed by 40 cycles at 95˚C for 15 sec, annealing at 60˚C for 30 sec and elongation at 72˚C for 1 min; and final extension at 72˚C for 5 min. The expression levels of ZEB1, interleukin (IL)-6, IL-1β, and tumour necrosis factor (TNF)-α were normalised to glyceraldehyde 3-phosphate dehydrogenase and calculated with the $2^{-\Delta\Delta Cq}$ method (29). The primer sequences used were as follows: ZEB1 forward, 5'-AGCAGTGAAAGAGAAGGGAATGC-3' and reverse, 5'-GGTCCTCTTCAGGTGCCTCAG-3'; IL-6 forward, 5'-TCCAGTTGCCTTCTTGGGAC-3' and reverse, 5'-GTACTCCAGAAGACCAGAGG-3'; IL-1β forward, 5'-CCAGCTTCAAATCTCACAGCAG-3' and reverse, 5'-CTTCTTTGGGTATTGCTTGGGATC-3'; TNF-α forward, 5'-CACAGAAAGCATGATCCGCGA-3' and reverse, 5'-CGGCAGAGAGGAGGTTGACTTTCT-3'.

*Western blotting.* The kidney tissues were lysed with radioimmunoprecipitation assay lysis buffer (Beyotime Institute of Biotechnology). The protein concentration was detected via BCA Protein Assay kit and 50 $\mu$g protein/lane was separated via 10% sodium dodecyl sulphate polyacrylamide gel electrophoresis and transferred onto nitrocellulose membranes. The membranes were blocked with 5% skim milk for 2 h at 25˚C and then incubated with the following primary antibodies: anti-ZEB1 (1:1,000; product code ab124512; Abcam), anti-AMPKα1 (1:1,000; product code ab32047), anti-phosphorylated (p)-AMPKα1 (1:1,000; product code ab92701), anti-mTOR (1:1,000; product code ab32028), anti-p-mTOR (1:1,000; product code ab109268), anti-caspase-9 (1:1,000; product code ab184786), anti-caspase-3 (1:1,000; product code ab13847), anti-microtubule-associated protein 1 light chain-3B (LC3B; 1:1,000; product code ab48394), anti-LC3A/B (1:1,000; product code ab62721), and anti-Beclin-1 (1:1,000; product code ab210498; all from Abcam) overnight at 4˚C. The membranes were subsequently incubated with the horseradish peroxidase-conjugated anti-mouse IgG secondary antibody (1:5,000; product code ab6728; Abcam) for 2 h at 25˚C. The protein blots were developed with an enhanced chemiluminescence kit (Invitrogen; Thermo Fisher Scientific, Inc.). Quantity One 1-D Analysis Software (Bio-Rad Laboratories, Inc.) was used to measure the density of the western blot bands.

*Statistical analysis.* All data were analysed using SPSS Statistics 23.0 software (IBM Corp.). Data were expressed as the mean ± standard deviation. One-way ANOVA followed by Tukey's post hoc test was used to evaluate the differences among multiple groups, whereas acute kidney damage score and sepsis score were analysed using the Kruskal-Wallis test and Dunn's multiple comparison test, respectively. P-values <0.05 were considered to indicate statistically significant differences. All experiments were performed in triplicate.

## Results

*ZEB1 expression is downregulated in CLP-induced AKI.* As observed from the results of the western blotting assay, the expression of the ZEB1 protein in the CLP group was significantly decreased compared with that in the blank group (P<0.01; Fig. 1A). In addition, the RT-qPCR results presented similar findings (P<0.01; Fig. 1B). The BUN and SCr levels in the CLP group were significantly enhanced compared with those in the blank group (P<0.01; Fig. 1C). Compared with the blank group, the sepsis score in the CLP group was also increased (P<0.01; Fig. 1D). Furthermore, pathological changes of the kidney tissues were observed under a light microscope. The kidney tubules and glomerulus structures were normal in the sham group. Telangiectasia and severe congestion were observed in the kidney tissues of the CLP group (Fig. 1E). The acute kidney damage score of the CLP group was higher than that of the blank group (P<0.01; Fig. 1F). In addition, several other kidney injury-related parameters were measured. As presented in Table I, urine volume and urine sodium were significantly increased, whereas urine osmolality, MAP, and RBF were decreased in the CLP group compared with the blank group (P<0.01).

*Autophagy and the AMPK/mTOR pathway are blocked in CLP-induced AKI.* Western blot analysis revealed that the expression levels of the autophagy marker proteins Beclin-1 and LC3A/B were significantly decreased in the CLP group compared with the blank group (P<0.01; Fig. 2A). In addition, the protein expression of p-AMPK/AMPK was decreased while

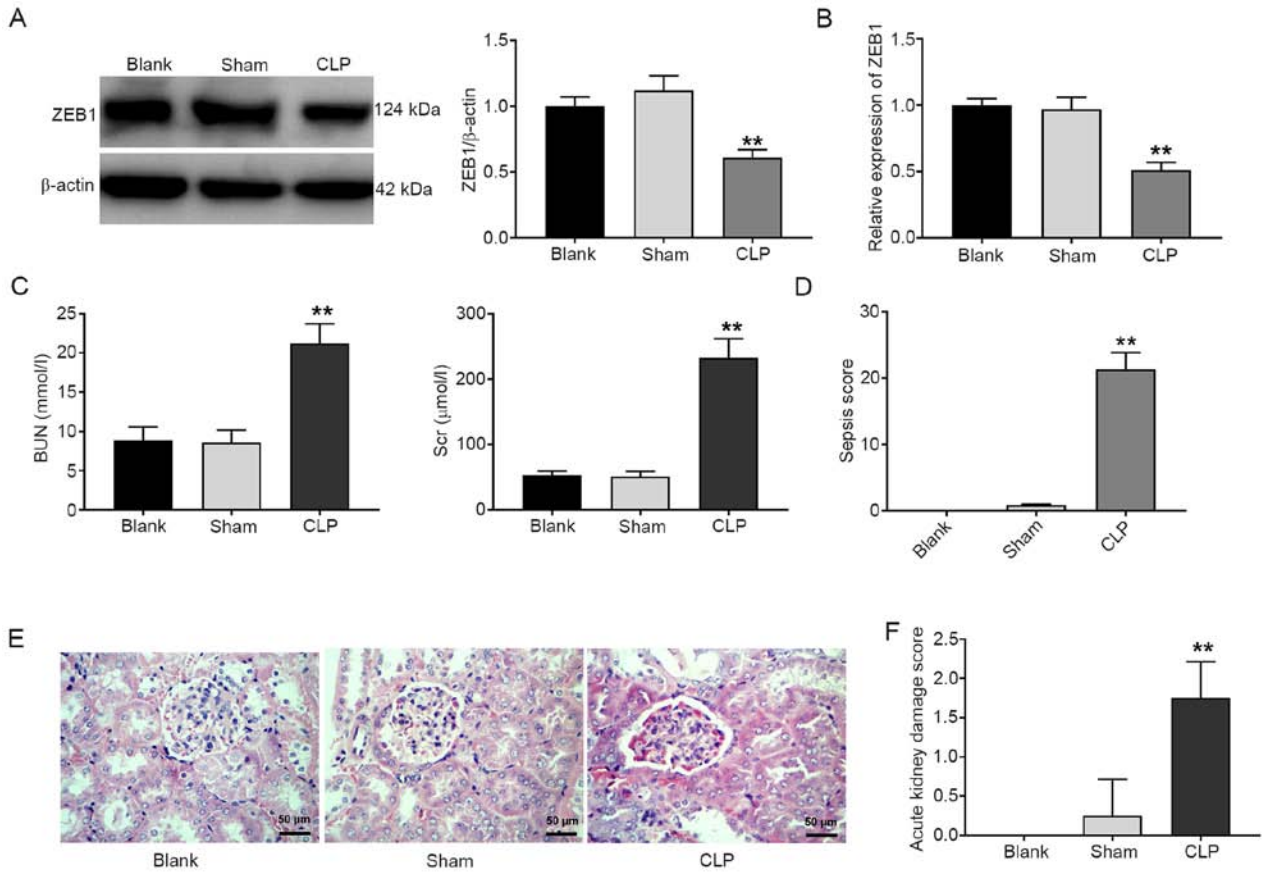


Figure 1. ZEB1 expression and pathological characteristics in CLP-induced AKI rats. (A) Western blot analysis of ZEB1 expression in kidney tissues. (B) Reverse transcription-quantitative polymerase chain reaction analysis of ZEB1 expression in kidney tissues. (C) The levels of BUN and SCr in rats. (D) The sepsis score in rats. (E) Pathological changes of renal tissues observed by hematoxylin and eosin staining (scale bar, 50 $\mu$m). (F) Acute kidney damage score in rats. Blank, normal rats; Sham, rats underwent laparotomy and bowel manipulation without CLP; CLP, rats underwent CLP. $^{**}$P<0.01 compared with the blank group. The data are presented as the mean ± SD of 3 independent experiments. ZEB1, zinc-finger E-box-binding homeobox 1; CLP, cecal ligation and puncture; AKI, acute kidney injury; BUN, blood urea nitrogen; SCr, serum creatinine.

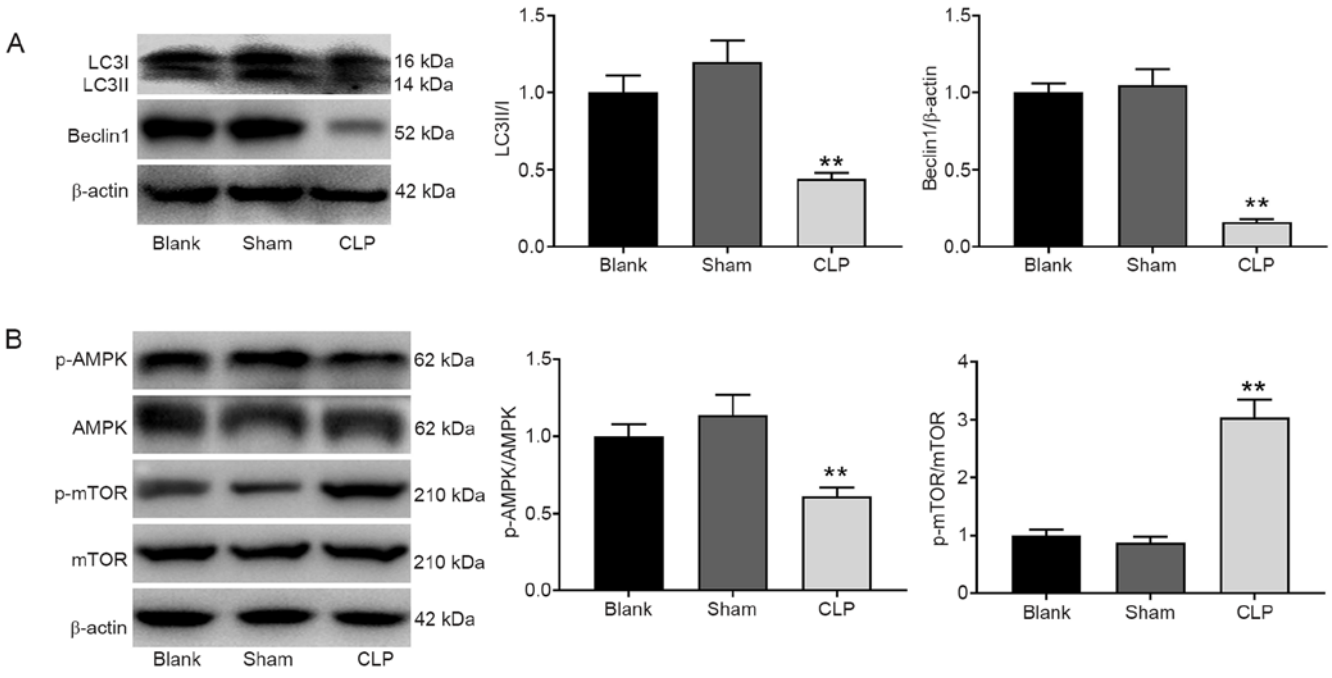


Figure 2. Autophagy and the AMPK/mTOR pathway are blocked in CLP-induced AKI. (A) Western blot analysis of Beclin1 and LC3II/I expression in kidney tissues. (B) Western blot analysis of p-AMPK/AMPK and p-mTOR/mTOR expression in kidney tissues. Blank, normal rats; Sham, rats underwent laparotomy and bowel manipulation without CLP; CLP, rats underwent CLP. $^{**}$P<0.01 compared with the blank group. The data are presented as the mean ± SD of 3 independent experiments. AMPK, AMP-activated protein kinase; mTOR, mammalian target of rapamycin; CLP, cecal ligation and puncture; p-, phosphorylated.

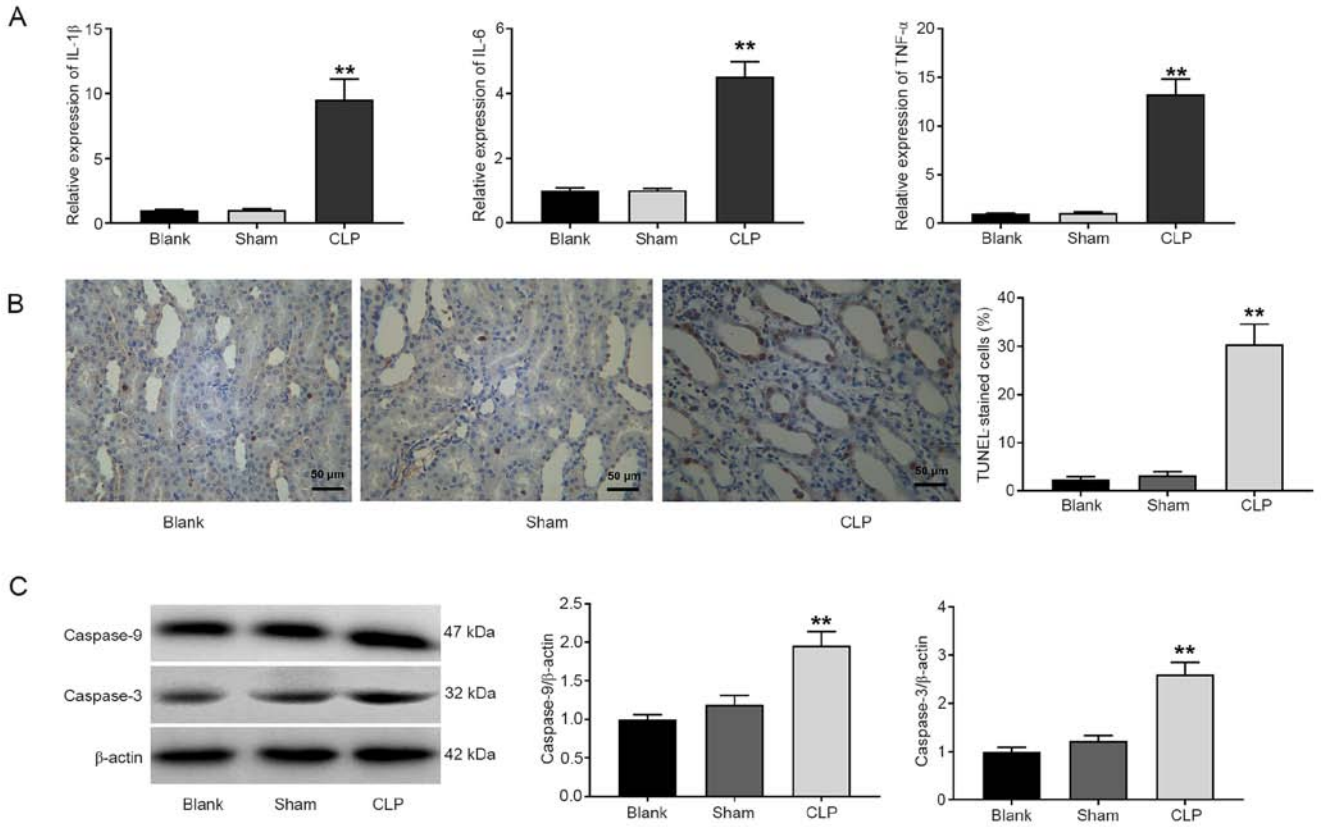


Figure 3. Inflammation and apoptosis are enhanced in CLP-induced AKI. (A) Reverse transcription-quantitative polymerase chain reaction analysis of the levels of IL-6, IL-1β, and TNF-α. (B) TUNEL staining of apoptosis in kidney tissues (scale bar, 50 $\mu$m). (C) Western blot analysis of caspase-9 and caspase-3 expression in kidney tissues. Blank, normal rats; Sham, rats underwent laparotomy and bowel manipulation without CLP; CLP, rats underwent CLP. $^{**}$P<0.01 compared with the blank group. The data are presented as the mean ± SD of 3 independent experiments. CLP, cecal ligation and puncture; AKI, acute kidney injury; IL, interleukin; TNF-α, tumour necrosis factor-α; TUNEL, terminal deoxynucleotidyl transferase dUTP nick end labeling.

the protein expression of p-mTOR/mTOR was increased in the CLP group compared with the blank group (P<0.01; Fig. 2B).

*Inflammation and apoptosis are enhanced in CLP-induced AKI.* As revealed in Fig. 3A, the expression levels of IL-1β, IL-6 and TNF-α in the CLP group were significantly increased compared with those in the blank group (P<0.01). An increased number of TUNEL-positive cells was observed in the CLP group compared with the blank group (P<0.01; Fig. 3B). The protein expression levels of caspase-9 and caspase-3 were also detected via western blotting. Compared with the blank group, the protein expression levels of caspase-9 and caspase-3 were significantly increased in the CLP group (P<0.01; Fig. 3C).

*Overexpression of ZEB1 activates the AMPK/mTOR pathway in CLP-induced AKI.* To validate whether ZEB1 participated in AKI by regulating the AMPK/mTOR pathway, the protein expression levels of ZEB1, p-AMPK/AMPK, and p-mTOR/mTOR were detected after injection of Ad-ZEB1 and DM into CLP-induced AKI rats. The protein expression of ZEB1 was significantly increased in the CLP + Ad-ZEB1 group compared with the CLP group (P<0.01; Fig. 4A). Similarly, through RT-qPCR analysis, increased ZEB1 expression was detected in the CLP + Ad-ZEB1 group compared with the CLP group (P<0.01; Fig. 4B). As revealed in Fig. 4C, the expression of p-AMPK/AMPK was significantly increased while that of p-mTOR/mTOR was significantly decreased in the CLP + Ad-ZEB1 group compared with the CLP + Ad-NC group (P<0.01). The effects of ZEB1 overexpression on the expression levels of p-AMPK/AMPK and p-mTOR/mTOR were significantly reversed by DM.

*Overexpression of ZEB1 alleviates AKI and enhances autophagy in CLP-induced AKI.* The role of ZEB1 in CLP-induced AKI and autophagy was further evaluated. As presented in Fig. 5A-C, the BUN and SCr levels, acute kidney damage score, and sepsis score were significantly decreased by ZEB1 overexpression in CLP-induced AKI (P<0.01). The inhibitory effect of ZEB1 overexpression on AKI was eliminated by DM (P<0.01). In addition, according to the histopathological changes presented in Fig. 5B, it was observed that overexpression of ZEB1 obviously attenuated the damage (telangiectasia and severe congestion) of CLP on the kidney tubules and glomerulus. However, treatment with DM reversed this condition. The expression levels of the autophagy-related proteins Beclin-1 and LC3A/B were measured via western blotting. Overexpression of ZEB1 significantly increased the expression levels of LC3A/B and Beclin-1 in CLP-induced AKI (P<0.01). DM reversed the effect of ZEB1 overexpression on the autophagy of CLP-induced AKI (P<0.01; Fig. 5D).

*Overexpression of ZEB1 inhibits inflammation and apoptosis in CLP-induced AKI.* The effects of ZEB1 on inflammation and cell apoptosis in CLP-induced rats were measured. Compared with the CLP + Ad-NC group, the expression levels

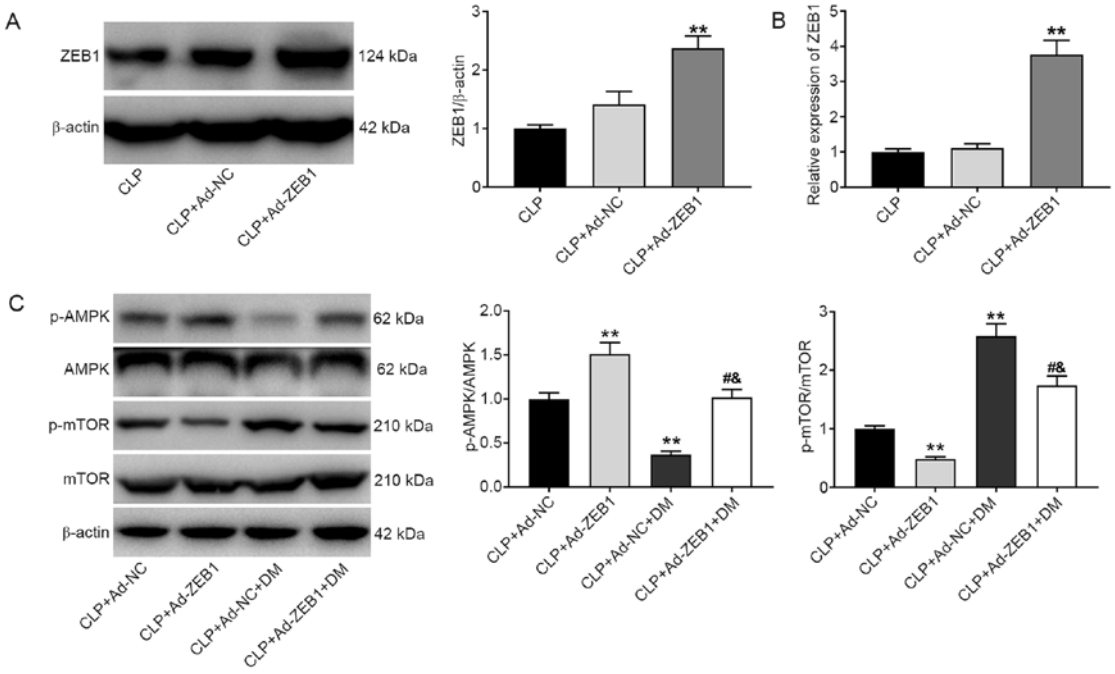


Figure 4. ZEB1 overexpression activates the AMPK/mTOR signaling pathway in CLP-induced AKI. (A) Western blot analysis of ZEB1 expression in kidney tissues. (B) Reverse transcription-quantitative polymerase chain reaction analysis of ZEB1 expression in kidney tissues. (C) Western blot analysis of p-AMPK/AMPK and p-mTOR/mTOR expression in kidney tissues. CLP + Ad-NC, rats were caudally injected with Ad-NC before CLP. CLP + Ad-ZEB1, rats were caudally injected with Ad-ZEB1 before CLP. CLP + Ad-NC + DM, rats were intravenously injected with Ad-NC caudally and intraperitoneally injected with AMPK inhibitor DM before CLP. CLP + Ad-ZEB1 + DM, rats were intravenously injected with Ad-ZEB1 caudally and intraperitoneally injected with DM before CLP. $^{**}$P<0.01 vs. CLP or CLP + Ad-NC group; $^{\#}$P<0.05 compared with CLP + Ad-ZEB1 group; $^{\&}$P<0.05 vs. CLP + Ad-NC + DM group. The data are presented as the mean ± SD of 3 independent experiments. ZEB1, zinc-finger E-box-binding homeobox 1; AMPK, AMP-activated protein kinase; mTOR, mammalian target of rapamycin; CLP, cecal ligation and puncture; AKI, acute kidney injury; p-, phosphorylated; DM, dorsomorphin.

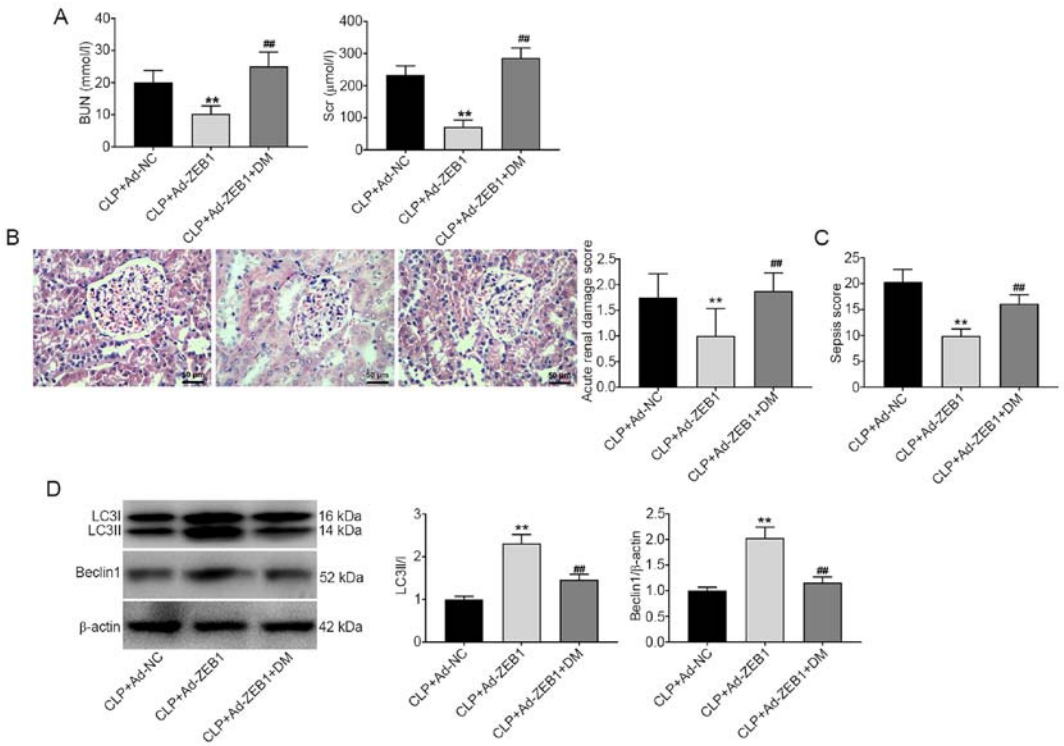


Figure 5. ZEB1 overexpression alleviates AKI and enhances autophagy in CLP-induced AKI. (A) The levels of BUN and SCr in rats. (B) Pathological changes of renal tissues observed by hematoxylin and eosin staining (scale bar, 50 $\mu$m) and the acute kidney damage score of rats. (C) The sepsis score in rats. (D) Western blotting analysis of Beclin1 and LC3II/I expression in kidney tissues. CLP + Ad-NC, rats were intravenously injected with Ad-NC caudally before CLP. CLP + Ad-ZEB1, rats were intravenously injected with Ad-ZEB1 caudally before CLP. CLP + Ad-ZEB1 + DM, rats were intravenously injected with Ad-ZEB1 caudally and intraperitoneally injected with DM before CLP. $^{**}$P<0.01 compared with the CLP + Ad-NC group; $^{\#\#}$P<0.01 compared with the CLP + Ad-ZEB1 group. The data are presented as the mean ± SD of 3 independent experiments. ZEB1, zinc-finger E-box-binding homeobox 1; AKI, acute kidney injury; CLP, cecal ligation and puncture; BUN, blood urea nitrogen; SCr, serum creatinine; DM, dorsomorphin.

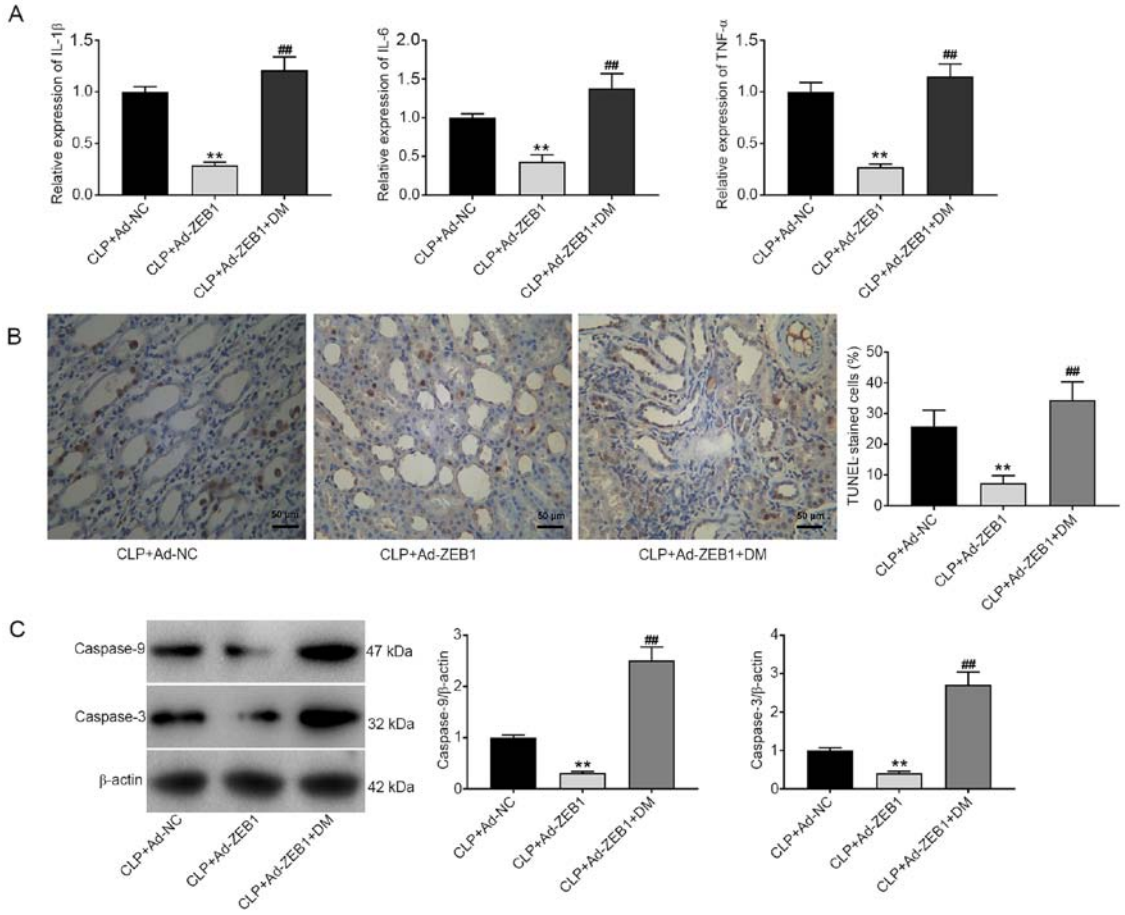


Figure 6. ZEB1 overexpression inhibits the inflammation and apoptosis in CLP-induced AKI. (A) Reverse transcription-quantitative polymerase chain reaction analysis of the levels of IL-6, IL-1β and TNF-α in kidney tissues. (B) TUNEL staining of apoptosis in kidney tissues (scale bar, 50 $\mu$m). (C) Western blot analysis of caspase-9 and caspase-3 expression in kidney tissues. CLP + Ad-NC, rats were intravenously injected with Ad-NC caudally before CLP. CLP + Ad-ZEB1, rats were intravenously injected with Ad-ZEB1 caudally before CLP. CLP + Ad-ZEB1 + DM, rats were intravenously injected with Ad-ZEB1 caudally and intraperitoneally injected with DM before CLP. $^{**}$P<0.01 compared with the CLP + Ad-NC group; $^{\#\#}$P<0.01 compared with the CLP + Ad-ZEB1 group. The data were presented as the mean ± SD of 3 independent experiments. ZEB1, zinc-finger E-box-binding homeobox 1; CLP, cecal ligation and puncture; AKI, acute kidney injury; IL, interleukin; TNF-α, tumour necrosis factor-α; DM, dorsomorphin; TUNEL, terminal deoxynucleotidyl transferase dUTP nick end labeling.

of IL-1β, IL-6 and TNF-α were significantly reduced in the CLP + Ad-ZEB1 group (P<0.01; Fig. 6A). Conversely, DM recovered the expression levels of IL-6, IL-1β, and TNF-α that were reduced by ZEB1 overexpression (P<0.01). The cell apoptosis and protein expression levels of caspase-9 and caspase-3 were detected via TUNEL and western blotting. The number of TUNEL-positive cells and the expression levels of caspase-9 and caspase-3 were decreased in the CLP + Ad-ZEB1 group compared with the CLP + Ad-NC group (P<0.01). The inhibitory effect of ZEB1 overexpression on cell apoptosis was reversed by intraperitoneal injection of DM (P<0.01; Fig. 6B and C).

## Discussion

Sepsis is the most common cause of AKI in critical patients and is recognised as the foremost precipitant of AKI (30,31). At present, *in vivo* experiments are the primary means of basic research on sepsis. Animal models can effectively simulate the pathological process of sepsis and can be conducive to elucidating the pathogenesis of AKI in humans (32). In the present study, the AKI model was evaluated by analysing BUN, SCr, acute kidney damage score, urine volume, urine osmolality, urine sodium, MAP, and RBF. The data revealed that the acute kidney damage score, BUN level, SCr level, urine volume, and urine sodium were higher while urine osmolality, MAP, and RBF were lower in the CLP group than those in the blank group. These results indicated that CLP induced severe kidney injury and that the rat AKI model was successfully established.

Autophagy is an essential pathway for the maintenance of cellular homeostasis and the response to stress, and dysregulation of autophagy is involved in the pathogenesis of numerous diseases (33-38). Growing evidence has revealed that autophagy protects the kidneys from various kidney inflammatory insults (39,40). Eva-1 homolog A-mediated autophagy was revealed to weaken liver injury in acute liver failure mice by attenuating inflammatory responses and apoptosis (41). The inhibition of autophagy was revealed to aggravate apoptosis, inflammation, and oxidative stress in the lung tissues of traumatic brain injury rats (42). Autophagy activation attenuated the levels of TNF-α and IL-6 in ischaemia reperfusion injury of the kidneys (43). In the present study, the results revealed that the expression levels of Beclin-1 and LC3A/B were significantly decreased in CLP rats. These data indicated that autophagy was blocked in the progression of AKI. It was

speculated that autophagy activation may relieve AKI by inhibiting cell apoptosis and inflammation.

A previous study revealed that ZEB1 expression was suppressed in hypoxia-induced cell injury (44). A similar result was observed in CLP-induced AKI. In the present study, the expression of ZEB1 was reduced in CLP-induced rats. In addition, it was revealed that ZEB1 overexpression decreased inflammation in CLP-induced AKI rats. This result is consistent with a previous study reporting that ZEB1 overexpression reduced the inflammation and brain damage caused by acute ischaemic stroke (24). Additionally, ZEB1 was overexpressed in AKI rats by injection of Ad-ZEB1 and it was revealed that overexpression of ZEB1 increased the expression levels of Beclin-1 and LC3A/B as well as inhibited inflammation and apoptosis in the kidney tissues of AKI rats. These results indicated that ZEB1 may relieve AKI by activating autophagy and inhibiting inflammation and apoptosis. Furthermore, in addition to the role of ZEB1 in autophagy, inflammation, and apoptosis, ZEB1 has been reported to be correlated with EMT progression (18,20,45). Xiong *et al* (20) revealed that ZEB1 was a transcriptional repressor of E-cadherin, which regulated the EMT of tubular epithelial cells. Because EMT plays a pivotal role in the process of renal fibrosis, it was hypothesised that ZEB1 may also influence AKI by regulating EMT. However, there is also a potential limitation in this study. The time-course expression profiles of ZEB1 were not measured in kidney tissues of AKI rats after injection of Ad-ZEB1. The optimal action time of Ad-ZEB1 still needs to be determined.

The AMPK/mTOR pathway is widely involved in the development of numerous diseases, including inflammation, cardiac dysfunction, and AKI (17,46-48). The present study revealed that the AMPK/mTOR pathway was blocked in CLP-induced AKI rats. Overexpression of ZEB1 activated the AMPK/mTOR pathway in CLP-induced AKI rats. In addition, the injection of the AMPK inhibitor DM reversed the protective effect of ZEB1 on CLP-induced AKI. These results indicated that ZEB1 overexpression relieved CLP-induced AKI by activating the AMPK/mTOR pathway. A previous study revealed that preconditioning mice with an AMPK activator ameliorated ischaemic AKI *in vivo* (47). The protective effect of curcumin on LPS-induced acute lung injury was exerted via AMPK activation (49). Thus, it was speculated that ZEB1-mediated activation of the AMPK/mTOR pathway may contribute to AKI remediation.

In conclusion, ZEB1 alleviated CLP-induced AKI in rats by activating autophagy as well as inhibiting inflammation and apoptosis. The protective effect of ZEB1 overexpression on AKI was achieved via activation of the AMPK/mTOR pathway. The present findings indicated that ZEB1 may be a potential therapeutic target for AKI. However, further research is required to identify the role of autophagy and the underlying mechanisms in AKI.

**Acknowledgements**

Not applicable.

**Funding**

No funding was received.

**Availability of data and materials**

The datasets used and/or analyzed during the current study are available from the corresponding author on reasonable request.

**Authors' contributions**

All authors contributed to the study conception and design. Material preparation, data collection and analysis were performed by XL, LZ and BZ. The first draft of the manuscript was written by DS. DS and BZ authenticated all the raw data. All authors were involved in writing and revising, as well as reading and approving the final manuscript.

**Ethics approval and consent to participate**

All experimental protocols were approved by the Ethics Committee of The First Affiliated Hospital of Shandong First Medical University. All procedures were performed in accordance with ethical standards and laboratory care and use guidelines of the First Affiliated Hospital of Shandong First Medical University.

**Patient consent for publication**

Not applicable.

**Competing interests**

The authors declare that they have no competing interests.

**References**

1. Makris K and Spanou L: Acute kidney injury: Definition, pathophysiology and clinical phenotypes. Clin Biochem Rev 37: 85-98, 2016.
2. Chen H and Busse LW: Novel therapies for acute kidney injury. Kidney Int Rep 2: 785-799, 2017.
3. Wafaisade A, Lefering R, Bouillon B, Sakka SG, Thamm OC, Paffrath T, Neugebauer E and Maegele M; Trauma Registry of the German Society for Trauma Surgery: Epidemiology and risk factors of sepsis after multiple trauma: An analysis of 29,829 patients from the Trauma Registry of the German Society for Trauma Surgery. Crit Care Med 39: 621-628, 2011.
4. Arulkumaran N, Sixma ML, Jentho E, Ceravola E, Bass PS, Kellum JA, Unwin RJ, Tam FW and Singer M: Sequential analysis of a panel of biomarkers and pathologic findings in a resuscitated rat model of sepsis and recovery. Crit Care Med 45: e821-e830, 2017.
5. Cho S, Lee YJ and Kim SR: Acute peritoneal dialysis in patients with acute kidney injury. Perit Dial Int 37: 529-534, 2017.
6. Ueno T: The roles of continuous renal replacement therapy in septic acute kidney injury. Artif Organs 41: 667-672, 2017.
7. Kaushal GP and Shah SV: Autophagy in acute kidney injury. Kidney Int 89: 779-791, 2016.
8. Kundu M and Thompson CB: Autophagy: Basic principles and relevance to disease. Annu Rev Pathol 3: 427-455, 2008.
9. Srivastava RK, Traylor AM, Li C, Feng W, Guo L, Antony VB, Schoeb TR, Agarwal A and Athar M: Cutaneous exposure to lewisite causes acute kidney injury by invoking DNA damage and autophagic response. Am J Physiol Renal Physiol 314: F1166-F1176, 2018.
10. Mei S, Livingston M, Hao J, Li L, Mei C and Dong Z: Autophagy is activated to protect against endotoxic acute kidney injury. Sci Rep 6: 22171, 2016.
11. Leventhal JS, Ni J, Osmond M, Lee K, Gusella GL, Salem F and Ross MJ: Autophagy limits endotoxemic acute kidney injury and alters renal tubular epithelial cell cytokine expression. PLoS One 11: e0150001, 2016.

12. Kim J, Kundu M, Viollet B and Guan KL: AMPK and mTOR regulate autophagy through direct phosphorylation of Ulk1. Nat Cell Biol 13: 132-141, 2011.
13. He J, Deng L, Liu H, Chen T, Chen S, Xia S and Liu Y: BCL2L10/BECN1 modulates hepatoma cells autophagy by regulating PI3K/AKT signaling pathway. Aging (Albany NY) 11: 350-370, 2019.
14. Liu Y, Ren Z, Li X, Zhong J, Bi Y, Li R, Zhao Q and Yu X: Pristimerin induces autophagy-nediated cell death in K562 cells through the ROS/JNK signaling pathway. Chem Biodivers 16: e1900325, 2019.
15. Wang K, Chu D, Wu J, Zhao M, Zhang M, Li B, Du W, Du J and Guo R: WITHDRAWN: Cinobufagin induced cell apoptosis and protective autophagy through the ROS/MAPK signaling pathway. Life Sci: Jul 11, 2019 (Epub ahead of print). doi: 10.1016/j.lfs.2019.116642.
16. Li K, Liu T-X, Li J-F, Ma YR, Liu ML, Wang YQ, Wu R, Li B, Shi LZ and Chen C: rhEPO inhibited cell apoptosis to alleviate acute kidney injury in sepsis by AMPK/SIRT1 activated autophagy. Biochem Biophys Res Commun 517: 557-565, 2019.
17. Zhao W, Zhang L, Chen R, Lu H, Sui M, Zhu Y and Zeng L: SIRT3 protects against acute kidney injury via AMPK/mTOR-regulated autophagy. Front Physiol 9: 1526, 2018.
18. Comijn J, Berx G, Vermassen P, Verschueren K, van Grunsven L, Bruyneel E, Mareel M, Huylebroeck D and van Roy F: The two-handed E box binding zinc finger protein SIP1 downregulates E-cadherin and induces invasion. Mol Cell 7: 1267-1278, 2001.
19. Thiery JP, Acloque H, Huang RY and Nieto MA: Epithelial-mesenchymal transitions in development and disease. Cell 139: 871-890, 2009.
20. Xiong M, Jiang L, Zhou Y, Qiu W, Fang L, Tan R, Wen P and Yang J: The miR-200 family regulates TGF-β1-induced renal tubular epithelial to mesenchymal transition through Smad pathway by targeting ZEB1 and ZEB2 expression. Am J Physiol Renal Physiol 302: F369-F379, 2012.
21. Furuya M, Masuda H, Hara K, Uchida H, Sato K, Sato S, Asada H, Maruyama T, Yoshimura Y, Katabuchi H, *et al*: ZEB1 expression is a potential indicator of invasive endometriosis. Acta Obstet Gynecol Scand 96: 1128-1135, 2017.
22. Sultan and Aneesa: Functional characterization of the transcription factor ZEB1 in epithelial to mesenchymal transition and cancer progression. (Unpublished PhD thesis). University of Vienna, 2010.
23. Bui T, Sequeira J, Wen TC, Sola A, Higashi Y, Kondoh H and Genetta T: ZEB1 links p63 and p73 in a novel neuronal survival pathway rapidly induced in response to cortical ischemia. PLoS One 4: e4373, 2009.
24. Li D, Lang W, Zhou C, Wu C, Zhang F, Liu Q, Yang S and Hao J: Upregulation of microglial ZEB1 ameliorates brain damage after acute ischemic stroke. Cell Rep 22: 3574-3586, 2018.
25. Siles L, Ninfali C, Cortés M, Darling DS and Postigo A: ZEB1 protects skeletal muscle from damage and is required for its regeneration. Nat Commun 10: 1364, 2019.
26. Rittirsch D, Huber-Lang MS, Flierl MA and Ward PA: Immunodesign of experimental sepsis by cecal ligation and puncture. Nat Protoc 4: 31-36, 2009.
27. Shrum B, Anantha RV, Xu SX, Donnelly M, Haeryfar SM, McCormick JK and Mele T: A robust scoring system to evaluate sepsis severity in an animal model. BMC Res Notes 7: 233, 2014.
28. Leelahavanichkul A, Yasuda H, Doi K, Hu X, Zhou H, Yuen PS and Star RA: Methyl-2-acetamidoacrylate, an ethyl pyruvate analog, decreases sepsis-induced acute kidney injury in mice. Am J Physiol Renal Physiol 295: F1825-F1835, 2008.
29. Livak KJ and Schmittgen TD: Analysis of relative gene expression data using real-time quantitative PCR and the 2(-Delta Delta C(T)) method. Methods 25: 402-408, 2001.
30. Hoste EA, Bagshaw SM, Bellomo R, Cely CM, Colman R, Cruz DN, Edipidis K, Forni LG, Gomersall CD, Govil D, *et al*: Epidemiology of acute kidney injury in critically ill patients: the multinational AKI-EPI study. Intensive Care Med 41: 1411-1423, 2015.
31. Gomez H and Kellum JA: Sepsis-induced acute kidney injury. Curr Opin Crit Care 22: 546-553, 2016.
32. Huan JN: Recognizing prevention and treatment of burn sepsis with the concept of holistic integrative medicine. Zhonghua Shao Shang Za Zhi 33: 196-199, 2017 (In Chinese).
33. Croce KR and Yamamoto A: A role for autophagy in Huntington's disease. Neurobiol Dis 122: 16-22, 2019.
34. Galluzzi L, Bravo-San Pedro JM, Blomgren K and Kroemer G: Autophagy in acute brain injury. Nat Rev Neurosci 17: 467-484, 2016.
35. Feng L, Liao X, Zhang Y and Wang F: Protective effects on age-related macular degeneration by activated autophagy induced by amyloid-β in retinal pigment epithelial cells. Discov Med 27: 153-160, 2019.
36. Jia G, Cheng G and Agrawal DK: Autophagy of vascular smooth muscle cells in atherosclerotic lesions. Autophagy 3: 63-64, 2007.
37. Lipinski MM, Zheng B, Lu T, Yan Z, Py BF, Ng A, Xavier RJ, Li C, Yankner BA, Scherzer CR, *et al*: Genome-wide analysis reveals mechanisms modulating autophagy in normal brain aging and in Alzheimer's disease. Proc Natl Acad Sci USA 107: 14164-14169, 2010.
38. Singh R, Xiang Y, Wang Y, Baikati K, Cuervo AM, Luu YK, Tang Y, Pessin JE, Schwartz GJ and Czaja MJ: Autophagy regulates adipose mass and differentiation in mice. J Clin Invest 119: 3329-3339, 2009.
39. Lenoir O, Tharaux PL and Huber TB: Autophagy in kidney disease and aging: Lessons from rodent models. Kidney Int 90: 950-964, 2016.
40. Kimura T, Isaka Y and Yoshimori T: Autophagy and kidney inflammation. Autophagy 13: 997-1003, 2017.
41. Lin X, Cui M, Xu D, Hong D, Xia Y, Xu C, Li R, Zhang X, Lou Y, He Q, *et al*: Liver-specific deletion of Eva1a/Tmem166 aggravates acute liver injury by impairing autophagy. Cell Death Dis 9: 768, 2018.
42. Xu X, Zhi T, Chao H, Jiang K, Liu Y, Bao Z, Fan L, Wang D, Li Z, Liu N, *et al*: ERK1/2/mTOR/Stat3 pathway-mediated autophagy alleviates traumatic brain injury-induced acute lung injury. Biochim Biophys Acta Mol Basis Dis 1864: 1663-1674, 2018.
43. Ling H, Chen H, Wei M, Meng X, Yu Y and Xie K: The effect of autophagy on inflammation cytokines in renal ischemia/reperfusion injury. Inflammation 39: 347-356, 2016.
44. Shi K, Sun H, Zhang H, Xie D and Yu B: miR-34a-5p aggravates hypoxia-induced apoptosis by targeting ZEB1 in cardiomyocytes. Biol Chem 400: 227-236, 2019.
45. Chua HL, Bhat-Nakshatri P, Clare SE, Morimiya A, Badve S and Nakshatri H: NF-kappaB represses E-cadherin expression and enhances epithelial to mesenchymal transition of mammary epithelial cells: Potential involvement of ZEB-1 and ZEB-2. Oncogene 26: 711-724, 2007.
46. Zhang J, Zhao P, Quan N, Wang L, Chen X, Cates C, Rousselle T and Li J: The endotoxemia cardiac dysfunction is attenuated by AMPK/mTOR signaling pathway regulating autophagy. Biochem Biophys Res Commun 492: 520-527, 2017.
47. Lieberthal W, Tang M, Lusco M, Abate M and Levine JS: Preconditioning mice with activators of AMPK ameliorates ischemic acute kidney injury in vivo. Am J Physiol Renal Physiol 311: F731-F739, 2016.
48. Jeon SM: Regulation and function of AMPK in physiology and diseases. Exp Mol Med 48: e245, 2016.
49. Kim J, Jeong SW, Quan H, Jeong CW, Choi JI and Bae HB: Effect of curcumin (Curcuma longa extract) on LPS-induced acute lung injury is mediated by the activation of AMPK. J Anesth 30: 100-108, 2016.